



## Analysis for Mechanical Consequences of a Core Disruptive Accident in Prototype Fast Breeder Reactor

P.Chellapandi<sup>1)</sup>, K.Velusamy<sup>1)</sup>, S.C.Chetal<sup>1)</sup>, S B Bhoje<sup>1)</sup>, Harbans Lal<sup>2)</sup>, V.S.Sethi<sup>2)</sup>

1) Indira Gandhi Centre for Atomic Research, Kalpakkam-603 102, India

2) Terminal Ballistic Research Laboratory, Chandigarh-160 020, India.

### ABSTRACT

The mechanical consequences of a core disruptive accident (CDA) in a fast breeder reactor are described. The consequences are development of deformations and strains in the vessels, intermediate heat exchangers (IHX) and decay heat exchangers (DHX), impact of sodium slug on the bottom surface of the top shield, sodium release to reactor containment building through top shield penetrations, sodium fire and consequent temperature and pressure rise in reactor containment building (RCB). These are quantified for 500 MWe Prototype Fast Breeder Reactor (PFBR) for a CDA with 100 MJ work potential. The results are validated by conducting a series of experiments on 1/30<sup>th</sup> and 1/13<sup>th</sup> scaled down models with increasing complexities. Mechanical energy release due to nuclear excursion is simulated by chemical explosion of specially developed low density explosive charge. Based on these studies, structural integrity of primary containment, IHX and DHX is demonstrated. The sodium release to RCB is 350 kg which causes pressure rise of 12 kPa in RCB.

**KEY WORDS:** Core Disruptive Accident, Mechanical consequences, structural integrity of heat exchangers, sodium slug impact, sodium release to RCB, sodium fire in RCB, transient pressure loading to RCB, simulation of nuclear excursion.

### INTRODUCTION

Core Disruptive Accident (CDA) resulting in core melt down is a very low probability event in an FBR and hence it is considered as a Beyond Design Basis Event. Nevertheless to provide defense-in-depth (rather requirement associated with environmental impact assessments), an energy release of 100 MJ is considered for PFBR which is arrived at based on the reactor safety analysis [1]. Subsequently, analysis is carried out to ensure that the main vessel and its top shield, decay heat exchangers (DHX), intermediate heat exchangers (IHX) and reactor containment building (RCB) including reactor vault are integral. The transient forces for the RCB design are due to temperature and pressure rise resulting from burning of sodium released through the top shield.

The report provides the summary of analyses carried out to determine (i) deformations of reactor assembly components, (ii) transient forces on the reactor vault, (iii) sodium release to RCB through top shield penetrations and (iv) temperature and pressure rise in RCB.

### MECHANICAL CONSEQUENCES OF CDA

A CDA involves release of a large amount of energy at the core due to nuclear power excursion. This produces an energetic volume at the core center containing vapourised mixture of fuel, coolant and other structural materials, which is termed as 'core bubble'. The mechanical consequences are illustrated schematically in Fig.1.

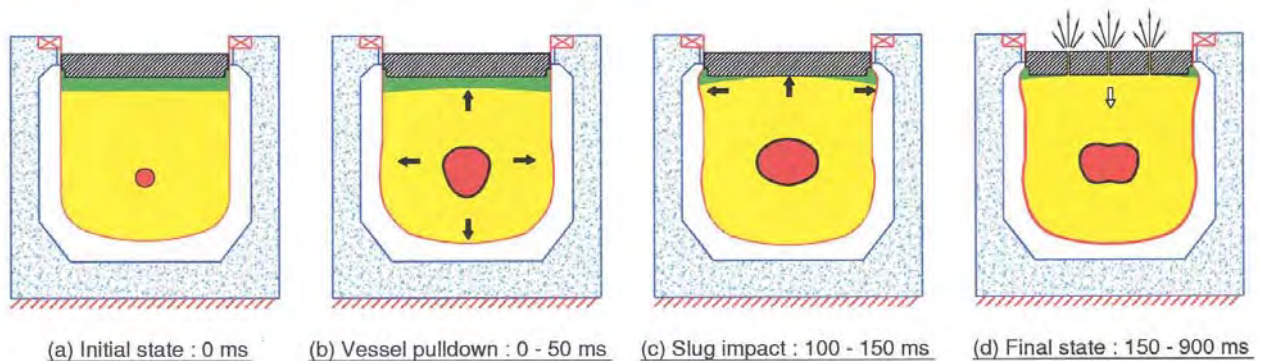


Fig.1 Mechanical consequences of CDA

### **Mechanical Energy Release**

The core bubble, not in equilibrium with the surrounding materials, expands by generating pressure waves in all directions. In the process of expansion, the bubble pressure is reduced and mechanical energy is released depending upon structure surrounding the bubble. If there is no constraint to its expansion up to 0.1 MPa, it can release its entire potential energy, which is called 'work potential' of the CDA. Fig.1a depicts the location of core bubble.

### **Deformations of Important Reactor Assembly Components**

An immediate effect of pressure waves generated by core bubble is plastic deformation of surrounding structures which offer resistance for the propagation of pressure waves. Due to the presence of cover gas space above the sodium free level, there is less resistance for the movement of liquid in the upward direction and hence, a portion of sodium above the bubble is accelerated upwards. Hence, a net force develops in the downward direction due to which, the main vessel is pulled-down. This in turn produces compressive force on the reactor vault, which is termed as 'pull-down force', and occurs during the initial stage of the accident, i.e. 0-50 ms in a typical pool type reactor. Fig.1b shows the deformation of the main vessel bottom under the pull-down force.

### **Sodium Slug Impact on Top Shield**

The accelerated sodium continues to move upward for a certain period (~50 ms) during which, there is no significant mechanical deformations, till sodium impacts on the top shield. Once the sodium impacts on the top shield, which is termed as 'sodium slug impact', the kinetic energy of the moving sodium is converted into pressure energy. Consequently, the pressure in the cover gas as well as in the sodium increases steeply, producing (i) further overall plastic deformation on the main vessel, (ii) large local deformation on the main vessel near top shield junction in the form of bulging and (iii) impact force on the top shield in the upward direction. The slug impact phenomenon (from the start of impact till stabilization of vessel deformation) occurs during 100-150 ms (Fig.1c).

### **Transient Forces on Reactor Vault**

The two important phases of the accident where the vault is subjected to forces are schematically illustrated in Fig.1b and Fig.1c respectively. In the first phase the reactor vault is pulled down by the main vessel through support shell, due to net unbalanced pressure force acting on the bottom portion, and in the second phase, it is subjected to upward force through top shield due to sodium slug impact. The force acting on the support shell which in turn transmits to the reactor vault is the net effect of these two forces.

### **Sodium Release to RCB**

During the slug impact, the bolts of top shield components elongate and the seals in the annular gaps of the top shield may fail. As a result of this, sodium may fill the top shield penetrations. Subsequently, sodium leaks to RCB. The leaked sodium catches fire and causes temperature and pressure rise in the RCB, for which the RCB is designed.

During the quasi-static condition when the sodium leak phenomenon occurs, the core bubble pressure drops. This is mainly due to the cooling of the bubble by the surrounding sub-cooled sodium which has high heat capacity, while the volume of the core bubble remains unchanged. The quasi-static condition prevails during 150-900 ms (Fig.1d).

### **Effects of Internals**

For illustrating the various phases, the reactor internals such core subassemblies (CSA), inner vessel, grid plate, core support structure (CSS), control plug, IHX and pumps were not considered in the previous discussions. These components contribute by changing (i) energy release, (ii) magnitudes of transient forces and (iii) duration of each major phenomenon, by virtue of their geometrical features, location and inertial characteristics. These effects are quantified in the present analysis.

## **ANALYSIS APPROACH FOR MECHANICAL CONSEQUENCES**

The equation of state (EOS) for the core bubble in the form of pressure versus volume relation along with the initial pressure and initial volume is provided by reactor physics calculations. The EOS is such that the integrated 'PdV' work during the expansion from the initial pressure to the final pressure of 0.1 MPa is 100 MJ. Subsequently analyses are done as follows:

### **Phase-I: Theoretical Analysis of Structural Responses**

Analyses for deformations of reactor assembly components, transient force on the reactor vault and transient pressure distribution on the bottom surface of top shield are carried out by an axisymmetric finite element in-house computer code called 'FUSTIN'. FUSTIN solves a set of governing differential equations of fluid, structure and fluid-structure interaction dynamics written in ALE coordinates system. Mathematical modeling details of FUSTIN code are

described in ref [2]. FUSTIN has been validated based on many international benchmark problems. The validation details are described in ref [3]. Further, validations were done (described in phase-IV) by an elaborate experimental program carried out at Terminal Ballistic Research Laboratory (TBRL), Chandigarh.

Since the FUSTIN is an axisymmetric code, the 3D aspects and consequently the dynamic forces on DHX and IHX are not simulated accurately, even though the resistance offered by the pumps and IHX for the radial flow is accounted by placing an axisymmetric homogeneous porous structure. Hence, at the moment, the structural integrity of IHX and DHX is demonstrated through experimental route based on 1/13<sup>th</sup> scale mockup tests which are described subsequently.

### Phase-II: Sodium Release to RCB

The transient pressure developed at the top shield bottom due to sodium slug impact is responsible for the sodium release. The scenario involves: (i) elongation of hold down bolts of the components mounted on the top shield, (ii) failure of argon seal and establishment of leak paths in the top shield penetrations, (iii) replacement of argon in the penetrations by the sodium slug which marks the end of transient phase and start of a quasi-static condition, (iv) sodium leak to RCB during the quasi-static condition during which the sodium pressure in the pool is in static equilibrium with the core bubble pressure and (v) termination of sodium leak once the sodium pressure falls below the atmospheric value.

The quasi-static condition is defined by Phase-I analysis when the core bubble pressure is approximately equal to the cover gas pressure after slug impact phenomenon which is the starting pressure for the quasi-static condition. Subsequently analysis is carried out using SOSPIIL, an in-house program developed for the estimation of sodium leak during quasi static condition. The sodium pressure decays during the quasi static condition due to the presence of sub-cooled sodium pool surrounding the core bubble (~1200 t at ~ 823 K which can absorb the entire thermal energy released under CDA with a marginal temperature rise of ~2 K in the pool) and also due to ejection of sodium. In the SOSPIIL the following pressure decay characteristic,  $P_r(t)$  is adopted from the similar formulations used for FFTF analysis [4 ]:

$$P_r = ( P_o x e^{-t/\tau} ) V_o / ( V_o + Q ) \quad (1)$$

where  $P_o$  is the initial pressure and  $V_o$  is the initial volume of the core bubble for the quasi-static condition.  $Q$  is the instantaneous volume of the sodium released to RCB at any instant  $t$ .

The equations that govern the velocity of sodium leak are based on the balance between the acceleration of sodium mass in various sections of the penetrations, frictional and form resistances for flow through these penetrations and downward gravitational force of the sodium. In SOSPIIL, the frictional pressure drop,  $(\Delta P)_{friction}$  for the fluid motion has been estimated from the correlation ,

$$(\Delta P)_{friction} = ( 0.0032 + 0.221 / Re^{0.237} ) (L/D) (\rho V^2/2) \quad (2)$$

where  $Re$  is the Reynolds number,  $L$  is the frictional length,  $D$  is the hydraulic diameter,  $\rho$  is the density of the fluid and  $V$  is the fluid velocity. The governing equations and validation details of SOSPIIL can be found in ref [5].

### Phase-III: Temperature and Pressure Rise in RCB

The output from the SOSPIIL code i.e. sodium leak versus time is the input data for the estimation of temperature and pressure rise in RCB. This is carried out by a pool fire code SOFIRE II developed by ANL. The details of code and validations are presented in ref [6].

### Phase-IV: Experimental Investigations

The tests were carried out at TBRL in 3 stages. In the first stage under TRIG-I series, 17 tests were conducted in water filled cylindrical shells with rigid and fixed top and bottom plates of various dimensions to characterize the chemical charges (the energy conversion ratio, i.e. mechanical energy release per unit mass and the equation of state). In the second stage under TRIG-II series, tests were conducted in the main vessel models without any internals. Under this series, 30 tests on 1/30<sup>th</sup> scale models and 3 tests on 1/13<sup>th</sup> scale models were conducted. Sufficient data have been generated for validating the FUSTIN code and also for establishing acceptable strain limits for the vessels under simulated CDA loading conditions. In the last stage, under TRIG-III, tests were conducted on 1/13<sup>th</sup> scale mockups with the main purpose of demonstrating the structural integrity of IHX and DHX and also to estimate the sodium leak based on simulation principles. Totally 61 tests were completed during a period of 4 years.



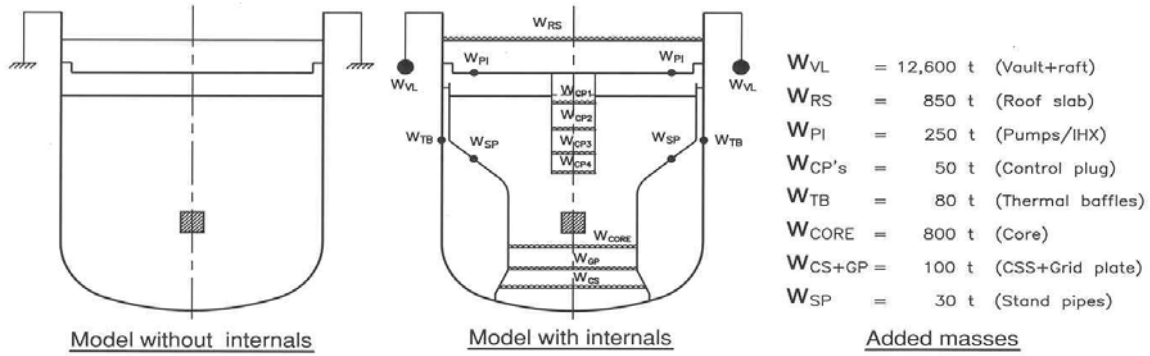


Fig.4 Idealised models used for CDA analysis

### Basic input data

The core bubble is modeled as a cylinder of diameter 1.47 m and height of 1.47 m with an initial volume  $V_0 = 2.5 \text{ m}^3$ , initial pressure  $P_0 = 4 \text{ MPa}$ . Equations of state for core bubble is:  $P = P_0 (V_0/V)^\gamma$  (MPa) where  $\gamma = 0.72$  and for sodium:  $P = 4.44 \times 10^9 \mu + 4.328 \times 10^9 |\mu| + 1.218 \times E(1+\mu)$ , where  $\rho_0 = 832 \text{ kg/m}^3$  and  $E$  is energy per unit volume (MJ/ $\text{m}^3$ ) &  $\mu = (\rho/\rho_0 - 1)$  and for cover gas is:  $P = P_0 [(V_0/V)^{1.67} - 1]$ , where  $P_0 = 0.1 \text{ MPa}$ ,  $V_0 = 105 \text{ m}^3$ .

### Results

Analysis is carried for two cases, i.e. with and without internals upto 200 ms, which covers the entire transient phase. The expansion behaviour of the core bubble is depicted at 3 instants (0, 100 and 200 ms) in Fig.5 for case with internals.

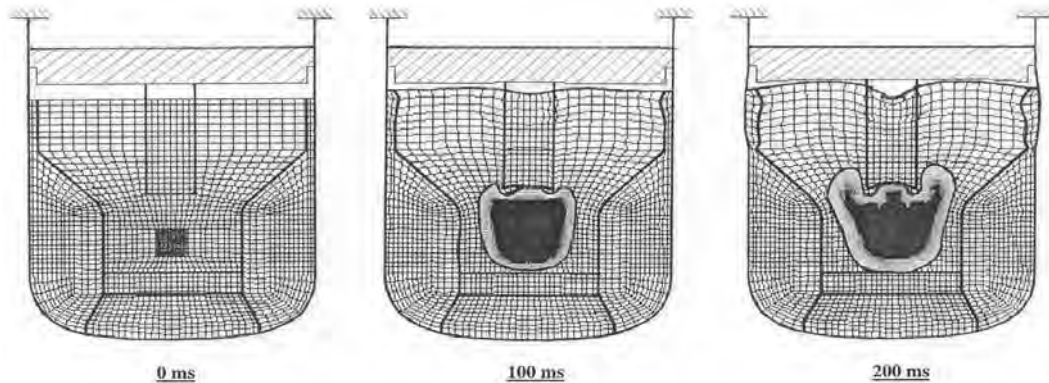


Fig.5 Evolution of core bubble

### Energy distributions

Even though the bubble has potential energy of 100 MJ, the actual energy release depends upon the constraints for the bubble expansion. The main vessel and the top shield offer constraints and hence the energy released is 65 MJ without internals. With the presence of internals, this value is reduced to ~ 55 MJ (Fig.6a). The energy absorbed by the main vessel is reduced significantly, i.e. from 55 to 25 MJ due to the presence of internals (Fig.6b).

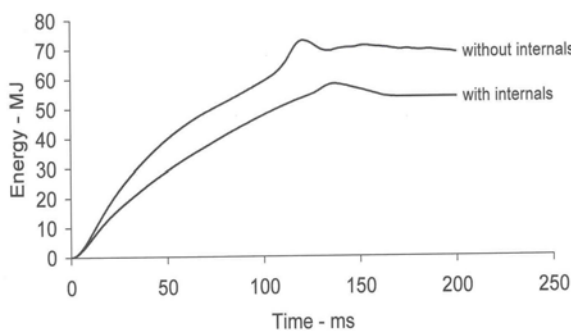


Fig.6a Core energy release

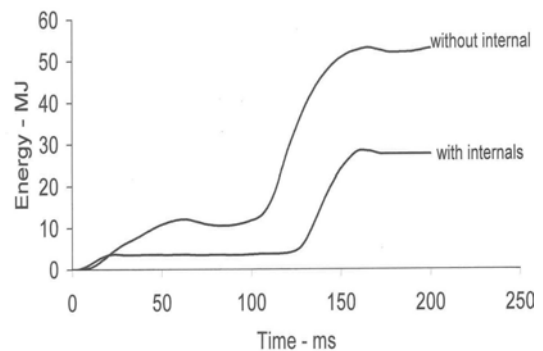


Fig.6b Energy absorbed by MV

**Permanent deformations in the main vessel**

The evolution of the main vessel bottom displacement as well as bulging of its upper portion is shown in Fig.7. The internals decrease the peak bottom displacement from 345 to 60 mm. Since the nominal gap between the main vessel and the safety vessel is 300 mm, with the inclusion of the internals, the main vessel does not touch the safety vessel. The maximum strain is 2.2 % which occurs at the upper portion of main vessel.

**Transient Forces on Reactor Vault**

The vault is subjected to transient forces (pull-down force transmitted by the main vessel and the impact force transmitted to the top shield) through the support shell, when the inertia of the top shield is ignored. If the masses of the top shield and the components supported on it are accounted, the net force transmitted to the vault decreases (Fig.8). If the internals are not included, the vault is subjected to ~ 131 MN tensile force and ~ 195 MN compressive force, which are high. But, by including the internals, no compressive force is imposed on the vault, apart from the dead load. The net tensile force is ~ 13 MN which is not very significant. If the reactor assembly is not anchored to the vault, it lifts up by ~ 5 mm under the tensile force. However, from seismic considerations, the reactor assembly is anchored to the vault and hence, the reactor assembly does not get lifted up. Thus, the effects of internals, which are mainly due to their geometrical features, location and inertial masses are significant that the net force transmitted to the vault is practically insignificant. This implies that the effects of CDA are negligible for the vault. More details on transient force on the reactor vault can be found in ref [8].

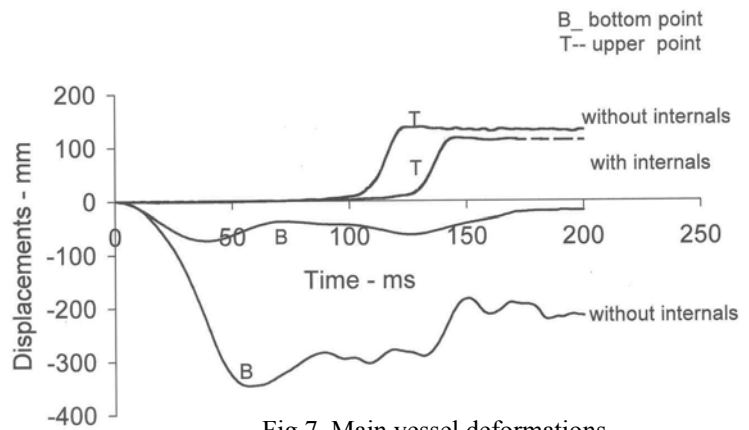


Fig.7 Main vessel deformations

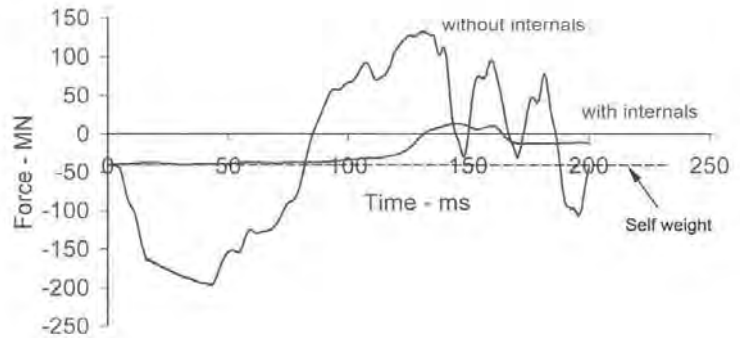


Fig.8 Transient force on vault

**Structural Integrity of Reactor Assembly Components : Experimental Studies**

Five tests were conducted with 22 g LDE which simulates 110 MJ of energy release in the reactor scale which is the design requirement. It is noted from the tests that the main vessel, top shield, DHX and IHX are integral with negligible deformations (Fig.9). It is worth mentioning that the tests with increasing quantity of LDE (up to 220 g) indicate that the main vessel without internals, is integral up to 1200 MJ (Fig.10).



Fig. 9 Removal of tested IHX



Fig.10 Deformed MV (1200 MJ case)

The maximum rupture strain is established as 30 % for welded SS 316 plates at room temperature under simulated CDA loadings. However, a strain limit of 16 % is considered (welded vessel) for PFBR at the operating temperature including the effects of multiaxiality, irradiation and accumulated creep-fatigue damage [9]. Strain measurements on the vault structure in the mockup confirmed the theoretical prediction of negligible force on the reactor vault for 100 MJ energy release.

## Sodium Release to RCB

### Theoretical prediction

Structural analysis of top shield and its components indicates that the hold down bolts of components, such as rotatable plugs, control plug, IHX, Primary Sodium Pump (PSP), DHX etc. undergo plastic elongation by 0.5 to 1 mm. With these input along with  $P_0$ , the starting value of quasi-static pressure (0.21 MPa),  $V_0$  the initial volume of the core bubble (81 m<sup>3</sup>), time constant  $\tau$  (0.8 s), the entry loss coefficient (0.5), the exit loss coefficient (1.0), the 90° bend loss coefficient (1.0), the sodium leak rate versus time is estimated by SOSPIIL code as shown in Fig.11. It is seen from Fig.11 that the total sodium leakage is ~ 350 kg.

### Experimental prediction

Water leak is measured in 1/13<sup>th</sup> scale mockup tests ( $Q_m$ ) and extrapolated to the reactor condition ( $Q_p$ ) using the equation (3). This equation is derived with assumptions: (i) negligible inertial and gravitational effects, (ii) smooth wall surfaces along the leak paths and (iii) pressure loss coefficient in the bend is independent of Reynolds number.

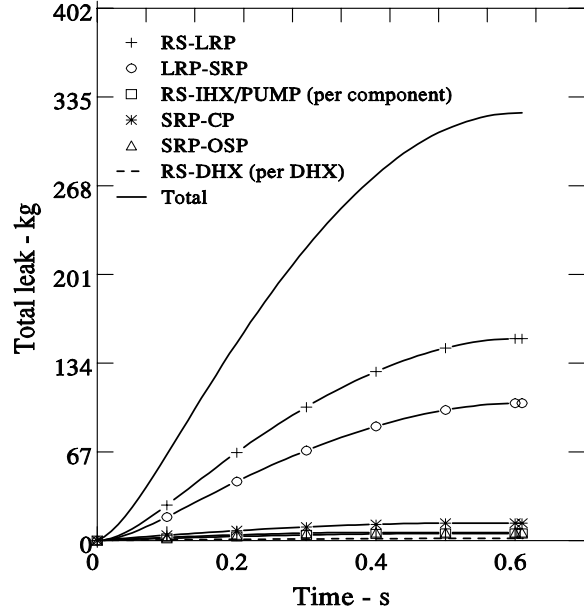


Fig.11 Sodium release

$$Q_p = Q_m \left( \frac{\rho_p}{\rho_m} \right)^{1/2} \left( \frac{A_p}{A_m} \right) \left( \frac{\Delta P_{0-quasi-p}}{\Delta P_{0-quasi-m}} \right)^{1/2} \left( \frac{\Delta T_p}{\Delta T_m} \right) \quad (3)$$

where,  $\rho$  is the density,  $A$  is the cross sectional flow area,  $\Delta P_{0-quasi}$  is the difference between the starting quasi-static pressure and atmospheric pressure,  $\Delta T$  is the duration of the quasi-static stage during which sodium release takes place and subscripts  $p$  and  $m$  refer to prototype and model.

In order to measure the water leak through the top shield annular penetrations, aluminum ducts filled with cotton (to absorb water) are used. By knowing the difference in weight of the ducts before and after the test, water leak through each path is quantified. The minimum and maximum quantity of water leaks measured in 5 experiments through all the penetrations which all simulate (110/13<sup>3</sup>) MJ of energy, is 1.75 and 2.415 kg. The maximum quantity of sodium leak in the reactor extrapolated through equation (3) is 233.2 kg. This value is ~ 70 % of theoretical prediction which shows the conservatism built in the numerical model.

### Temperature and Pressure Rise in RCB

Sodium release of 350 kg, the theoretically computed upper bound value, is taken as input for the estimation of temperature and pressure rise in RCB under CDA. Even though sodium ejection through the penetrations is a complex phenomenon, a simplified assumption is made for this part of calculation, wherein the entire sodium is assumed to get ejected out in horizontal direction (due to geometrical features of the penetrations), get collected as pool over top shield and burn. The event is analysed as a pool fire using SOFIRE II code. As 100% sodium monoxide as reaction product in diffusion controlled sodium fires can burn more sodium and give higher thermal consequences than 100% peroxide or any other ratios of oxides as reaction products, the same is considered for the analysis. Evolution of air temperature and pressure rise is shown in Fig.12a and 12b respectively. The peak gas temperature in RCB is estimated to be about 331 K and the peak pressure rise is about 9 kPa. Based on the information available on the prediction capability of SOFIRE II code, a factor of 1.3 is applied on the pressure rise in RCB [6]. Accordingly, the pressure rise of 12 kPa is considered as the maximum possible pressure rise in RCB due to a complete burning of 350 kg of sodium.

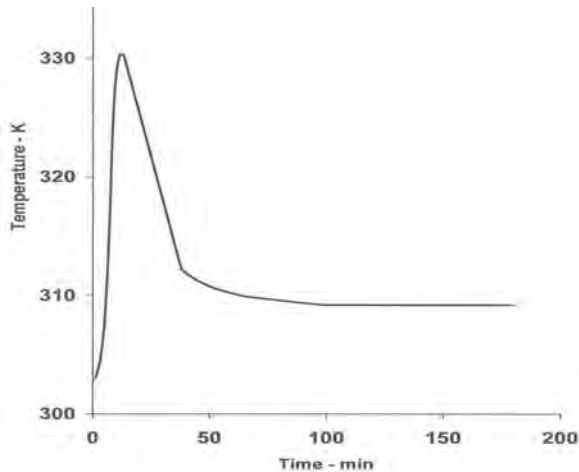


Fig.12a Temperature rise in RCB

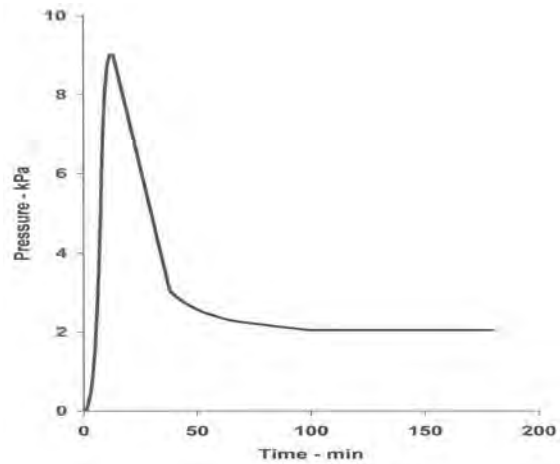


Fig.12b Pressure rise in RCB

## SUMMARY OF INVESTIGATIONS

Mechanical consequences of CDA involving 100 MJ energy release are investigated based on theoretical analyses using computer codes as well as 1/13<sup>th</sup> scale mockup tests. The computer codes used for the theoretical analysis have been validated extensively based on tests simulating CDA loading conditions. The following are the important results:

- The maximum main vessel strain predicted theoretically is 2.2 % which is much lower than the permissible value of ~16 % considered for PFBR. However, the rupture strains for SS316 welded plate at room temperature is established as 30 % based on many simulated tests with chemical explosion.
- The structural integrity of IHX and DHX is demonstrated based on mockup tests.
- The vault is subjected to negligible tensile as well as compressive forces. This has been confirmed with mockup tests.
- Theoretically computed upper bound sodium release through top shield penetrations is 350 kg. The conservatism in this value is demonstrated by mockup tests which indicate that the maximum and minimum quantities of sodium release are 170 kg and 234 kg respectively (extrapolated values).
- For the sodium release of 350 kg, the estimated values for the maximum temperature and pressure rise in RCB are 28 K and 12 kPa respectively.

## REFERENCES

1. Srinivasan, G.S. et al., "Core Disruptive Accident Analysis", Internal Report, PFBR/01117/DN/1012, 1999.
2. Chellapandi, P., "FUSTIN: A Code for Structural Analysis of Primary Containment under CDA: Mathematical Modeling", Internal Report RPFBR/31050/DN/1016, 2000.
3. Chellapandi, P., "FUSTIN Code Validation for Structural Analysis of Primary Containment", Internal Report, PFBR/31050/DN/1017, 2000
4. Stepnewski, D.D., et al., "Mechanical Consequences of Hypothetical Core Disruptive Accident", HEDL-TME 71-50, 1971.
5. Chellapandi, P., "SOSPIL: A Code for Estimating Sodium Release to RCB under CDA", Internal Report PFBR/31050/DN/1019, 2001.
6. Beiriger, P., and Hopenfeld, J., "SOFIRE II User Report", Atomics International Division, Rockwell International, AI-AEC-13055, 1979.
7. Chellapandi, P., "Structural Integrity Assessment of Primary Containment under CDA", Internal Report PFBR/31050/DN/1015, 1999.
8. Chellapandi, P., "Transient Loads on PFBR Reactor Vault under CDA", Proc. Workshop on Safety of Nuclear Power Plant Structures (SNPP-2001), Bangalore, 2001.
9. Kaguchi, H. et al., "Strain Limits for Structural Integrity Assessment of Fast Reactors under CDA", Proc. ICONE-7, Tokyo, Japan, 1999.

\* \* \*